Oleylamine as Both Reducing Agent and Stabilizer in a Facile Synthesis of Magnetite Nanoparticles

Zhichuan Xu,[†,‡] Chengmin Shen,[‡] Yanglong Hou,*[,§] Hongjun Gao,*[,‡] and Shouheng Sun*[,†]

Department of Chemistry, Brown University, Providence, Rhode Island 02912, Beijing National Laboratory for Condensed Matter Physics, Institute of Physics, Chinese Academy of Sciences, Beijing, China 100080, and College of Engineering, Peking University, Beijing, China 100871

Received November 1, 2008
Revised Manuscript Received March 26, 2009

Nanostructured magnetite (Fe_3O_4) has been one of the most attractive nanomaterials for various magnetic applications because of its chemical stability[1] and biocompability.[2] It is known that Fe_3O_4 nanoparticles (NPs) with controlled shapes are appealing for information storage applications,[3] and those coated with hydrophilic polymers have shown great potentials for medical diagnosis[4] and drug delivery.[5] Important progress has been made regarding wet chemical synthesis of Fe_3O_4 NPs[6] to meet an increasing demand for obtaining uniform NPs with tunable chemical and magnetic properties. Among all the sythetic procedures developed thus far, the thermal decomposition of iron acetylacetonate, $Fe(acac)_3$, in a high boiling point organic solvent in the presence of a reducing reagent and surfactants was first demonstrated to be an effective way to synthesize monodisperse Fe_3O_4 NPs.[6a] Further studies showed that the thermal decomposition of iron−oleate complex can produce monodiseprse Fe_3O_4 NPs in an ultra-large scale.[6b] Although this thermal decomposition method has become the main approach to high quality Fe_3O_4 NPs, the mechanism leading to the chemical conversions into Fe_3O_4 is complicated by the multicomponent reactants present in the reaction mixture. To meet a demand beyond the laboratory-scale production, a more reliable and simplified synthetic technique to Fe_3O_4 NPs with a better stoichiometric control is still desired.

Scheme 1

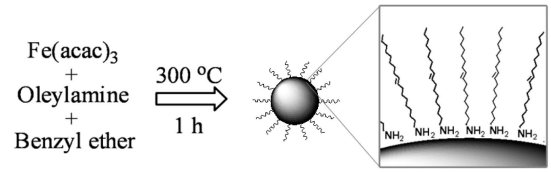

Recently, we reported a chemical synthesis of FeO NPs in the mixture of oleylamine and oleic acid.[7] By varying the heating conditions and ratios of oleylamine and oleic acid, the size of FeO NPs can be controlled from 14 to 100 nm. The experiment shows that the presence of excess amount of oleylamine is the key to provide a strong reductive environment for the thermal decomposition of $Fe(acac)_3$.[7] It indicates that oleylamine acts as an alternative reducing agent, which is inexpensive and even stronger than the 1,2-hexadecanediol that was used previously in the Fe_3O_4 NP synthesis.[6a] Taking advantage of multifunctional (reducing and capping) capabilities of oleylamine, we demonstrate here a much simplified organic phase synthesis of Fe_3O_4 NPs via the thermal decomposition of $Fe(acac)_3$ in benzyl ether and oleylamine, as illustrated in Scheme 1. By varying the volume ratio of benzyl ether and oleylamine, we can tune the NP sizes from 7 to 10 nm, a range that shows reasonably large magnetization and is suitable for a CVD catalytic study.

In a typical synthesis of ∼10 nm Fe_3O_4 NPs, $Fe(acac)_3$ (3 mmol) was dissolved in 15 mL of benzyl ether and 15 mL of oleylamine. The solution was dehydrated at 110 °C for 1 h under N_2 atmosphere, then quickly heated to 300 °C at a heating rate of 20 °C/min, and aged at this temperature for 1 h. After the reaction, the solution was allowed to cool down to room temperature. The Fe_3O_4 NPs were extracted upon the addition of 50 mL of ethanol, followed by centrifuging. The Fe_3O_4 NPs (yield ∼ 280 mg) were dispersed in nonpolar solvents such as hexane and toluene.

In the synthesis described above, the higer the ratio of oleylamine to benzyl ether, the smaller the Fe_3O_4 NPs. For example, ∼7 nm Fe_3O_4 NPs were obtained when only oleylamine was used. ∼8 and ∼9 nm Fe_3O_4 NPs were produced with the volume ratio of oleylamine to benzyl ether of 20:10 and 18:12, respectively. If the volume ratio of oleylamine to benzyl ether was less than 1:1, the Fe_3O_4 NPs with a broad size distribution were produced. This is probably due to the insufficiency of capping during the particle growth. The transmission electron microscopy (TEM) images of Fe_3O_4 NPs with different sizes are shown in Figure 1. It can be seen that the size distribution in each size group of the Fe_3O_4 NPs is very narrow. The corresponding size-distribu-

* Corresponding authors. E-mail: hou@pku.edu.cn; hjgao@aphy.iphy.ac.cn; ssun@brown.edu.
† Brown University.
‡ Chinese Academy of Sciences.
§ Peking University.

(1) (a) Zhao, M.; Beauregard, D. A.; Loizou, L.; Davletov, B.; Brindle, K. M. *Nat. Med.* **2001**, *7*, 1241. (b) Perez, J. M.; Josephson, L.; O'Loughlin, T.; Hogemann, D.; Weissleder, R. *Nat. Biotechnol.* **2002**, *20*, 816.
(2) (a) Tiefenauer, L. X.; Kuhne, G.; Andres, R. Y. *Bioconjugate Chem.* **1993**, *4*, 347. (b) Huh, Y. M.; Jun, Y.; Song, H. T.; Kim, S.; Choi, J.; Lee, J. H.; Yoon, S.; Kim, K. S.; Shin, J. S.; Suh, J. S.; Cheon, J. *J. Am. Chem. Soc.* **2005**, *127*, 12387.
(3) (a) Son, S. J.; Reichel, J.; He, B.; Schuchman, M.; Lee, S. B. *J. Am. Chem. Soc.* **2005**, *127*, 7316. (b) Zhao, W.; Gu, J.; Zhang, L.; Chen, H.; Shi, J. *J. Am. Chem. Soc.* **2005**, *127*, 8916.
(4) (a) Lee, J. H.; Huh, Y. M.; Jun, Y. W.; Seo, J. W.; Jang, J. T.; Song, H. T.; Kim, S. J.; Cho, E. J.; Yoon, H. G.; Suh, J. S.; Cheon, J. W. *Nat. Med.* **2007**, *13*, 95. (b) Seo, W. S.; Lee, J. H.; Sun, X. M.; Suzuki, Y.; Mann, D.; Liu, Z.; Terashima, M.; Yang, P. C.; Mcconnell, M. V.; Nishimura, D. G.; Dai, H. J. *Nat. Mater.* **2006**, *5*, 971.
(5) (a) Son, S. J.; Reichel, J.; He, B.; Schuchman, M.; Lee, S. B. *J. Am. Chem. Soc.* **2005**, *127*, 7316. (b) Zhao, W.; Gu, J.; Zhang, L.; Chen, H.; Shi, J. *J. Am. Chem. Soc.* **2005**, *127*, 8916.
(6) (a) Sun, S.; Zeng, H. *J. Am. Chem. Soc.* **2002**, *124*, 8204. (b) Park, J.; An, K.; Hwang, Y.; Park, J. G.; Noh, H. J.; Kim, J. Y.; Park, J. H.; Hwang, N. M.; Hyeon, T. *Nat. Mater.* **2004**, *3*, 891. (c) Yang, T.; Shen, C.; Li, Z.; Zhang, H.; Xiao, C.; Chen, S.; Xu, Z.; Shi, D.; Li, J.; Gao, H. *J. Phys. Chem. B* **2005**, *109*, 23233. (d) Hui, C.; Shen, C.; Yang, T.; Bao, L.; Tian, J.; Ding, H.; Li, C.; Hao, H. *J. Phys. Chem. C* **2008**, *112*, 11336. (e) Park, J.; Lee, E.; Hwang, N.; Kang, M.; Kim, S. C.; Hwang, Y.; Park, J. G.; Noh, H. J.; Kim, J. Y.; Park, J. H.; Hyeon, T. *Angew. Chem., Int. Ed.* **2005**, *44*, 2872.
(7) Hou, Y.; Xu, Z.; Sun, S. *Angew. Chem., Int. Ed.* **2007**, *46*, 6329.

10.1021/cm802978z CCC: $40.75
Published on Web 04/14/2009

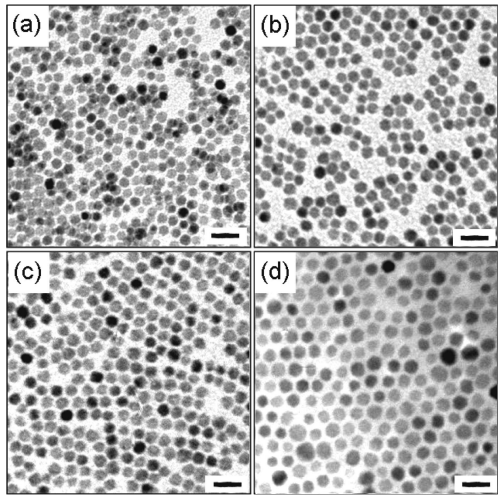

Figure 1. TEM images of Fe_3O_4 NPs: (a) 7 ± 0.5 nm, (b) 8 ± 0.4 nm, (c) 9 ± 0.6 nm, and (d) 10 ± 0.8 nm. Scale bar is 20 nm.

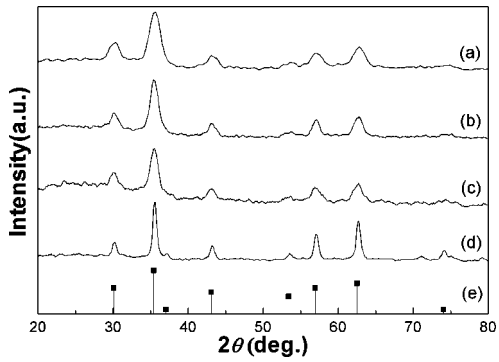

Figure 2. XRD patterns of Fe_3O_4 NPs: (a) ~7 nm, (b) ~8 nm, (c) ~9 nm. and (d) ~10 nm. (e) The standard Fe_3O_4 diffraction peaks (JCPDS 07-322).

tion histograms are given in Figure S1 (Supporting Information).

X-ray diffraction (XRD) was used to record the crystal infomation of Fe_3O_4 NPs. Figure 2 shows the XRD patterns of the Fe_3O_4 NPs at different sizes. The position and relative intensity of all diffraction peaks match well with the standard Fe_3O_4 peaks. The half-peak width of Fe_3O_4 NP decreases with the increase of NP sizes. The average NP sizes esitimated using Scherrer's formula[8] from each pattern are constant with the sizes observed in the TEM study, which indicates that each individual Fe_3O_4 NP is a single crystal.[6a,2] More importantly, the calculated lattice parameters from XRD patterns are 8.378, 8.381, 8.385, and 8.391 Å for ~7, ~8, ~9, and ~10 nm particles, respectively. They are quite close to the standard lattice parameter of magnetite (8.396 Å) and relatively far from the one of maghemite (8.346 Å), which indicates that the as-synthesized iron oxide particles are in magnetite phase.[9a,b] The little differences between the calculated lattice parameters and standard one are probably due to the small size induced surface instability of the oxygen stoichiometry of products.[9b,c] Chemically, these Fe_3O_4 NPs were also converted into γ-Fe_2O_3 (maghemite) and α-Fe_2O_3 (hematite) NPs in the controlled thermal annealing conditions (Figure S2, Supporting Information), indicating Fe_3O_4 is indeed formed during the synthesis.[9d]

The magnetic properties of the Fe_3O_4 NPs were studied using a vibrating sample magnetometer (VSM) at room temperature. All the Fe_3O_4 NPs exhibited superparamagnetic properties with slight differences in saturation magnetization. A typical hysteresis loop of the as-synthesized Fe_3O_4 NPs (~10 nm) is shown in Figure S3 (Supporting Information). The saturation moment of ~10 nm Fe_3O_4 NPs (including surfactant) is about 65 emu/g. To calculate the saturation moment of pure Fe_3O_4 NPs, the inductively coupled plasma mass spectrometry (ICP-MS) technique was used to determine the element content of Fe and Fe_3O_4. The ICP result showed that the weight percentage of Fe in gross particles is 58.8%, and correspondingly the weight percentage of Fe_3O_4 is 81.3%. It implies that the weight percentage of surfactant is about 18.7% in the particles. On the basis of the ICP analysis, the caculated saturation moment of the ~10 nm Fe_3O_4 NPs is ~80 emu/g, which is very close to the previously reported values measured from the Fe_3O_4 NPs in the similar size.[6a] In a similar way, the calculated saturation moments of ~9, ~8, and ~7 nm Fe_3O_4 NPs are ~79, ~77, and ~76 emu/g, respectively. This is consistent with the fact that the moment is dependent on the NP size and thermal agitation has only the minor effect on the moment reduction in this 7−10 nm NP size range.[9d]

The reductive thermal decomposition of $Fe(acac)_3$ into Fe_3O_4 NPs is different from that reported previously,[9d] in which a small amount of oleylamine was used with oleic acid together as surfactants and the 1,2-hexadecanediol was used as reducing reagent. In that synthesis, the product separated after a short refluxing time at reaction temperature (~300 °C) showed no magnetic response and contained FeO.[9d] However, in our current decomposition process, we found that the product separated from the reddish reaction solution at a relatively low temperature of 170 °C had a magnetic response, which indicates the existence of nucleated Fe_3O_4 nanocrystals. The TEM study (shown in Figure S4, Supporting Information) confirmed this assumption as small clusters (~2 nm) could be seen. The corresponding selected area electron diffraction (SAED) pattern showed weak but clear iron oxide spinel structure rings, indicating the formation of spinel structured iron oxide crystal clusters at this relatively low temperature. It is well-known that the presence of reducing reagent facilitates the thermal decomposition of metal complex at lower temperatures. For example, the decomposition of $Pt(acac)_2$ in the presence of a reducing reagent takes place as early as when 100 °C is reached,[10a,3] while without a reducing reagent its decomposition is delayed until 140 °C.[10b] This relatively low temperature decomposi-

(8) Klug, H. P.; Alexander, L. E. *X-ray Diffraction Procedures for Polycrystalline and Amorphous Materials*; John Wiley & Sons: New York, 1962; pp 491−538.

(9) (a) Belin, T.; Guigue-Millot, N.; Caillot, T.; Aymes, D.; Niepce, J. C. *J. Solid State Chem.* **2002**, *163*, 459. (b) Guigue-Millot, N.; Bégin-Colin, S.; Champion, Y.; Hïch, M. J.; Le Gaër, G.; Perriat, P. *J. Solid State Chem.* **2003**, *170*, 30. (c) Daou, T. J.; Pourroy, G.; Bégin-Colin, S.; Grenche, J. M.; Ulhaq-Bouillet, C.; Legar, P.; Bernhardt, P.; Leuvrey, C.; Rogez, G. *Chem. Mater.* **2006**, *18*, 4399. (d) Sun, S.; Zeng, H.; Robinson, D. B.; Raoux, S.; Rice, P. M.; Wang, S. X.; Li, G. *J. Am. Chem. Soc.* **2004**, *126*, 273.

(10) (a) Sun, S.; Murray, C. B.; Weller, D.; Folks, L.; Moser, A. *Science* **2000**, *287*, 1989. (b) Nandwana, V.; Elkins, K. E.; Liu, J. P. *Nanotechnology* **2005**, *16*, 2823.

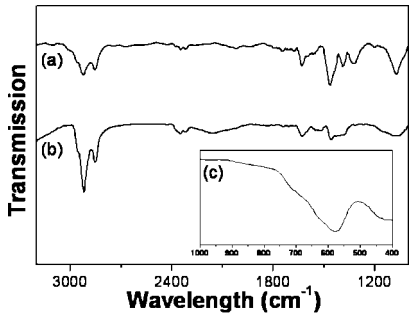

Figure 3. FT-IR spectra of (a) oleylamine and (b) as-synthesized Fe_3O_4 NPs. The inset (c) is the low frequency region of Fe_3O_4 NPs.

tion of $Fe(acac)_3$ is probably due to the existence of the excess amount of oleylamine, which gives an even stronger reductive environment compared with the one given by 1,2-hexadecanediol. This reductive environment provided by a large amount of oleylamine brought the decomposition temperature down to 170 °C, at which small spinel structured iron oxide crystals were directly produced rather than forming FeO species first at 300 °C.[9d]

The Fourier transform infrared (FT-IR) spectrum was used to characterize the surface chemistry and Fe−O bonds of the as-synthesized Fe_3O_4 NPs. Figure 3a,b shows the spectra of oleylamine and the NPs, respectively. The spectrum of Fe_3O_4 NPs is similar to the oleylamine one. For example, the bands in 1330−1650 cm^{-1} are due to $-NH_2$ bending mode, and the bands around 2920 cm^{-1} and 2850 cm^{-1} are for methyl stretching.[11] It should be noticed that the spectra a and b do not show the characteristic peak evolution from the amine group to the amide group as reported in the synthesis of Au NPs in the presence of oleylamine.[12] It indicates that there is no oxidized amide species capped on the surface of Fe_3O_4 NPs. Figure 3c shows the typical low frequency bands of spinel structured iron oxides, that is, the band at 578 cm^{-1} refers to Fe−O deformation in octahedral and tetrahedral sites and the band at 417 cm^{-1} refers to Fe−O deformation in octahedral sites.[9a]

One of the applications of these oleylamine capped monodisperse Fe_3O_4 NPs is to catalyze the growth of one-dimensional nanostructures in a chemical vapor deposition (CVD) system. The iron oxide NPs have been used as catalyst materials for the CVD based synthesis of carbon nanotubes[13] and boron nanowires.[14] In boron nanowire synthesis, the monodispersity of the NP catalyst is essential for the formation of the nanowires with a narrow diameter

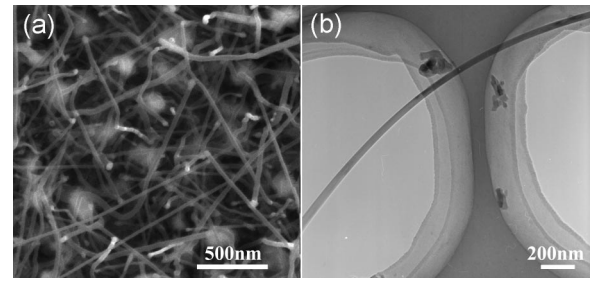

Figure 4. Typical SEM image of boron nanowires synthesized using oleylamine capped Fe_3O_4 NPs as catalyst (a) and the TEM image of a single boron nanowire (b).

distribution.[14a] To examine the catalysis of the oleylamine capped Fe_3O_4 NPs for the growth of boron nanowires, we deposited the ∼8 nm NPs from hexane on a silicon wafer as we described previously.[5] The wafer was put onto an alumina boat, in which a well-ground powder mixture of B_2O_3, B, and graphite in a mass ratio of 2:4:1 was loaded. The reaction was carried out at 1100 °C for 2 h in a gas mixture of 5% H_2 and 95% Ar. After being cooled to room temperature, a dark-brown product was found on the surface of the Si wafer. Figure 4a is the scanning electron microscopy (SEM) image of the nanowires prepared on the Si wafer, and Figure 4b is the TEM image of a single boron nanowire (boron nanowires were peeled off from the Si wafer and dispersed in the ethanol to sonicate for 20 min, and then two drops of this solution were dropped onto the carbon-coated copper grid and dried at room temperature). The nanowires are ∼30 nm in diameter and serveral micrometers in length. The wire dimensions are similar to that made from oleate/oleylamine coated Fe_3O_4 catalyst.[14] This indicates that our much simplified synthesis of Fe_3O_4 NPs should be the future choice for the mass production of Fe_3O_4 NPs for the catalytic growth of boron nanowires or other 1D nanostructures. The simple coating chemistry present on the surface of Fe_3O_4 NPs will also facilitate their surface functionalization for biomedical applications.

In summary, we have demonstrated a facile method to synthesize monodisperse Fe_3O_4 NPs via the reductive decomposition of $Fe(acac)_3$ in benzyl ether and oleylamine. In the synthesis, oleylamine acts both as a reducing agent and a stabilizer, and the particle size is controlled by varying the volume ratios of oleylamine and benzyl ether. The Fe_3O_4 NPs are a good catalyst for the CVD growth of boron nanowires. With their catalytic properties, their simple surface chemistry, and their superparamagnetism, these NPs should have great potential for large-scale CVD growth of novel 1D nanomaterials and for magnetic particle-based medical imaging and therapeutic applications.

Acknowledgment. The work was supported by NSF/DMR 0606264, National Science Foundation of China (Grants 60571045 and U0734003), and CAS/SAFEA international cooperation team.

Supporting Information Available: Fe_3O_4 nanoparticle characterizations (PDF). This material is available free of charge via the Internet at http://pubs.acs.org.

CM802978Z

(11) (a) Luo, J.; Han, L.; Kariuki, N. N.; Wang, L.; Mott, D.; Zhong, C. J.; He, T. *Chem. Mater.* **2005**, *17*, 5282. (b) Xie, J.; Xu, C.; Kohler, N.; Hou, Y.; Sun, S. *Adv. Mater.* **2007**, *19*, 3163.

(12) (a) Liu, X.; Atwater, M.; Wang, J.; Dai, Q.; Zou, J.; Brennan, J.; Huo, Q. *J. Nanosci. Nanotechnol.* **2007**, *7*, 3126. (b) Lattuada, M.; Hatton, T. A. *Langmuir* **2007**, *23*, 2158.

(13) (a) Oberlin, A.; Endo, M.; Koyama, T. *J. Cryst. Growth* **1976**, *32*, 335. (b) Su, M.; Zheng, B.; Liu, J. *Chem. Phys. Lett.* **2000**, *322*, 321. (c) Kong, J.; Cassell, A. M.; Dai, H. *Chem. Phys. Lett.* **1998**, *292*, 567.

(14) (a) Liu, F.; Tian, J.; Bao, L.; Yang, T.; Shen, C.; Lai, X.; Xiao, Z.; Xie, W.; Deng, S.; Chen, J.; She, J.; Xu, N.; Gao, H. *Adv. Mater.* **2008**, *20*, 2609. (b) Tian, J.; Cai, J; Hui, C.; Zhang, C.; Bao, L.; Gao, M.; Shen, C.; Gao, H. *Appl. Phys. Lett.* **2008**, *93*, 122105. (c) Wang, X.; Tian, J.; Yang, T.; Bao, L.; Hui, C.; Liu, F.; Shen, C.; Gu, C.; Xu, N.; Gao, H. *Adv. Mater.* **2007**, *19*, 4480.